

Solid versus Liquid Particle Sampling Efficiency of Three Personal Aerosol Samplers when Facing the Wind

KIRSTEN A. KOEHLER¹, T. RENEE ANTHONY², MICHAEL VAN DYKE³
and JOHN VOLCKENS^{1*}

¹Department of Environmental and Radiological Health Sciences, Colorado State University, Fort Collins, CO 80523-1681, USA; ²Department of Occupational and Environmental Health, University of Iowa, Iowa City, IA 52242, USA; ³Division of Environmental and Occupational Health Sciences, National Jewish Health, Denver, CO 80206, USA

Received 9 February 2011; in final form 15 July 2011; published online 29 September 2011

The objective of this study was to examine the facing-the-wind sampling efficiency of three personal aerosol samplers as a function of particle phase (solid versus liquid). Samplers examined were the IOM, Button, and a prototype personal high-flow inhalable sampler head (PHISH). The prototype PHISH was designed to interface with the 37-mm closed-face cassette and provide an inhalable sample at 10 l min^{-1} of flow. Increased flow rate increases the amount of mass collected during a typical work shift and helps to ensure that limits of detection are met, particularly for well-controlled but highly toxic species. Two PHISH prototypes were tested: one with a screened inlet and one with a single-pore open-face inlet. Personal aerosol samplers were tested on a bluff-body disc that was rotated along the facing-the-wind axis to reduce spatiotemporal variability associated with sampling supermicron aerosol in low-velocity wind tunnels. When compared to published data for facing-wind aspiration efficiency for a mouth-breathing mannequin, the IOM oversampled relative to mannequin facing-the-wind aspiration efficiency for all sizes and particle types (solid and liquid). The sampling efficiency of the Button sampler was closer to the mannequin facing-the-wind aspiration efficiency than the IOM for solid particles, but the screened inlet removed most liquid particles, resulting in a large underestimation compared to the mannequin facing-the-wind aspiration efficiency. The open-face PHISH results showed overestimation for solid particles and underestimation for liquid particles when compared to the mannequin facing-the-wind aspiration efficiency. Substantial (and statistically significant) differences in sampling efficiency were observed between liquid and solid particles, particularly for the Button and screened-PHISH, with a majority of aerosol mass depositing on the screened inlets of these samplers. Our results suggest that large droplets have low penetration efficiencies through screened inlets and that particle bounce, for solid particles, is an important determinant of aspiration and sampling efficiencies for samplers with screened inlets.

Keywords: aerosols; dust sampling conventions; exposure assessment; gravimetric analysis; inhalable dust

INTRODUCTION

A large body of literature exists regarding the sampling efficiency of personal samplers at varying wind speeds, orientations to the wind, and operating conditions for

solid particles (Kalatoor *et al.*, 1995; Kenny *et al.*, 1997; Roger *et al.*, 1998; Kenny *et al.*, 1999; Aizenberg *et al.*, 2000; Li *et al.*, 2000; Aizenberg *et al.*, 2001; Kennedy *et al.*, 2001; Paik and Vincent, 2004; Witschger *et al.*, 2004; Gorner *et al.* 2010). Yet, to our knowledge, only one laboratory study investigated droplet (i.e. liquid-phase particle) aspiration of the IOM (Institute of Occupational Medicine) sampler

*Author to whom correspondence should be addressed.
Tel: +970-491-6341; fax: +970-491-2941;
e-mail: john.volckens@colostate.edu

(SKC Inc., Eighty Four, PA, USA) (Zhou and Cheng, 2010). Although many occupational aerosol exposures involve solid particles, exposure to liquid-phase aerosol remains an area of concern for the occupational health community. Exposure to metal removal (metal-working) fluid aerosols is common, with reported mass median diameters ranging from 2.5 to 7.0 μm and geometric standard deviations often >2.5 (Piacitelli *et al.*, 2001). Droplet exposure also may occur during painting and other spraying operations, which often contain toxic anti-corrosives or solvents (Carlton, 2003; Glindmeyer *et al.*, 2004; Saby-Daily *et al.*, 2005). Printing processes (although likely comprised primarily submicron aerosol) and wet cleanup or pesticide application in agricultural activities (Amin *et al.*, 1999) may also result in workers' exposures to droplets.

The National Institute for Occupational Safety and Health (NIOSH) estimates that the number of workers in the USA exposed to metal removal fluid droplets may exceed 1 million (Sheehan, 1999). The health effects from exposure to metal removal fluids are significant and range from larynx, rectum, pancreas, skin, scrotum, or bladder cancers for straight oils to chronic respiratory diseases, including lipid pneumonia, hypersensitivity pneumonitis, asthma, acute airways irritation, and chronic bronchitis, for both straight and water-soluble oils (Wilsey *et al.*, 1996; NIOSH, 1998). To reduce potential health risks associated with metal removal fluid exposure, NIOSH recommends that exposures be limited to 0.4 mg m^{-3} for thoracic particulate mass or 0.5 mg m^{-3} for total particulate mass (as collected by a 'closed-face' 37-mm cassette, see below) for an 8-h exposure. In 2001, the American Conference of Governmental Industrial Hygienists (ACGIH) proposed an oil mist threshold limit value—8-h time-weighted average (TLV-TWA) of 0.2 mg m^{-3} measured as 'inhalable' aerosol; however, this TLV was withdrawn in 2010. Regulations based on an inhalable fraction are common in the UK and Europe. For example, the UK Health and Safety Executive (HSE) has suggested guidance values of 3 mg m^{-3} for oil-based and 1 mg m^{-3} for water-based metal removal fluids (Stear, 2003). Although this guidance value is not regulated, it is given as a recommendation to workplaces. Regulations are similar in other European countries: e.g. 8-h exposure limits, using inhalable sampling convention, of 1 mg m^{-3} in Sweden (Lillienberg *et al.*, 2010) and Austria (IFA, 2011) and 5 mg m^{-3} in Belgium (IFA, 2011). Although the USA has lagged Europe in the adoption and use of inhalable samplers, the ACGIH has recommended that all total particulate matter sampling regulations should be replaced by size-selective

physiologically relevant TLVs based on inhalable, thoracic, or respirable aerosol fractions (ACGIH, 2006). As such, it is important to understand the factors that determine the aspiration and sampling efficiency of inhalable aerosol samplers. The aspiration efficiency is the efficiency with which particles are transported from the ambient air into the inlet of a sampler (Paik and Vincent, 2004). The sampling efficiency is the efficiency with which particles are transported to the collection substrate (i.e. filter). The aspiration and sampling efficiencies are not necessarily equivalent as aspirated particles can deposit to the sampler walls (i.e. transmission losses) before reaching the substrate.

Currently in the USA, polystyrene 37-mm cassettes are commonly used to assess occupational exposure to aerosols. The cassette can be operated in either an 'open-face' or 'closed-face' configuration. The open-face configuration has a circular inlet of diameter nearly the width of the filter itself; the closed-face configuration has a reduced inlet diameter of 4 mm. Both these configurations are typically operated between 1 and 4 l min^{-1} of flow, with 2 l min^{-1} being the most common. While many studies have examined sampling efficiencies of 37-mm cassettes for solid particles (Kenny *et al.*, 1997; Kenny *et al.*, 1999; Witschger *et al.*, 2004; Gorner *et al.*, 2010), limited work has investigated liquid particle sampling efficiency. For droplet exposures, Beaulieu *et al.* (1980) reported that the open-face cassette collects $\sim 30\%$ more mass than the closed-face cassette. This difference, however, likely depends on particle size and composition as the concentration ratio measured between open- and closed-face cassettes ranged from 1.0 to 3.8 for other aerosol types. The ratio of the wind speed to the velocity of air through the inlet is also likely an important factor. Beaulieu *et al.* concluded that workers' exposures were probably being underestimated when assessed with a closed-face cassette. Other researchers have suggested that the open-face cassette is actually oversampling the aerosol (Buchan *et al.*, 1986). Several laboratory studies have measured orientation-averaged sampling efficiencies for the closed-face 37-mm cassette near 100% for 10 μm solid particles, but the sampling efficiencies dropped to below $\sim 20\%$ for particles $>40 \mu\text{m}$ for calm air conditions and at low wind speeds (Kenny *et al.*, 1997; Kenny *et al.*, 1999; Gorner *et al.*, 2010). Fewer studies have examined the sampling efficiency of 37-mm cassettes when facing-the-wind. Li *et al.* (2000) reported performances of closed-face 37-mm cassettes facing the wind at wind speeds of 0.55 and 1.1 m s^{-1} , which, when compared to mannequin aspiration efficiency reported by

Kennedy and Hinds (2002), slightly oversampled particles smaller than $\sim 20 \mu\text{m}$ but then sharply undersampled for larger particle sizes. Although the 37-mm cassette (open- or closed-face) does not meet any physiologically based size-selective sampling criteria, it remains one of the most common methods to assess aerosol exposures in the USA because this sampler is inexpensive, relatively easy to use, and disposable.

To address some of the limitations inherent with the 37-mm cassette, a personal high-flow inhalable sampler head (PHISH) was proposed and modeled by Anthony *et al.* (2010). The PHISH was designed to collect an inhalable sample at a higher flow (10 l min^{-1}) and interface with the existing 37-mm cassette. The increased flow rate, compared to other inhalable samplers (e.g. IOM sampler at 2 l min^{-1} or Button sampler at 4 l min^{-1}) was intended for application in low-concentration environments where increased sample mass is needed. The original PHISH design (which was subsequently modified as a result of this work, discussed below) consisted of a single 15-mm circular inlet hole covered with a 30-gage metal screen (30% open area, pore diameter of $254 \mu\text{m}$). The mesh screen was intended to prevent aspiration of larger particles ($>100 \mu\text{m}$) that are considered to be outside the inhalable size convention (ACGIH, 1999). To construct the screened PHISH, a metal washer (38 mm outer diameter, 15 mm inner diameter) was adhered into the inset of the middle

spacer of the 37-mm cassette with epoxy, flush with the leading edge. The metal screen was then adhered to the face of the washer with epoxy (Fig. 1a). Hence, the inlet face of the PHISH sampler was flat, in contrast to standard 37-mm three-piece cassettes. Additionally, all testing in the present study was performed with the PHISH inlet directly facing the wind, as opposed to the 30° downward angle that is typical when the standard 37-mm cassette is used as a personal sampler. This geometry requires that the PHISH must be attached to a holder to maintain proper alignment (Fig. 1).

Computational fluid dynamics simulations of the screened PHISH inlet indicated that solid particles (which are allowed to bounce off all surfaces) would be 'oversampled' up to 35% and liquid particles (which do not bounce) would be 'undersampled' between 50 and 95% under facing-the-wind conditions (0.4 m s^{-1} freestream velocity) for particle diameters between 5 and $100 \mu\text{m}$. The degree of over- and undersampling was defined relative to the facing-the-wind mannequin aspiration efficiency reported by Kennedy and Hinds (2002) (Anthony *et al.*, 2010). From these simulations, Anthony *et al.* concluded that oversampling occurred as a result of particle bounce at or around the screened inlet (for solid aerosol) and undersampling occurred by droplet deposition onto the screen itself. Consequently, we chose to investigate the sampling efficiency of the PHISH operating with and without the mesh screen

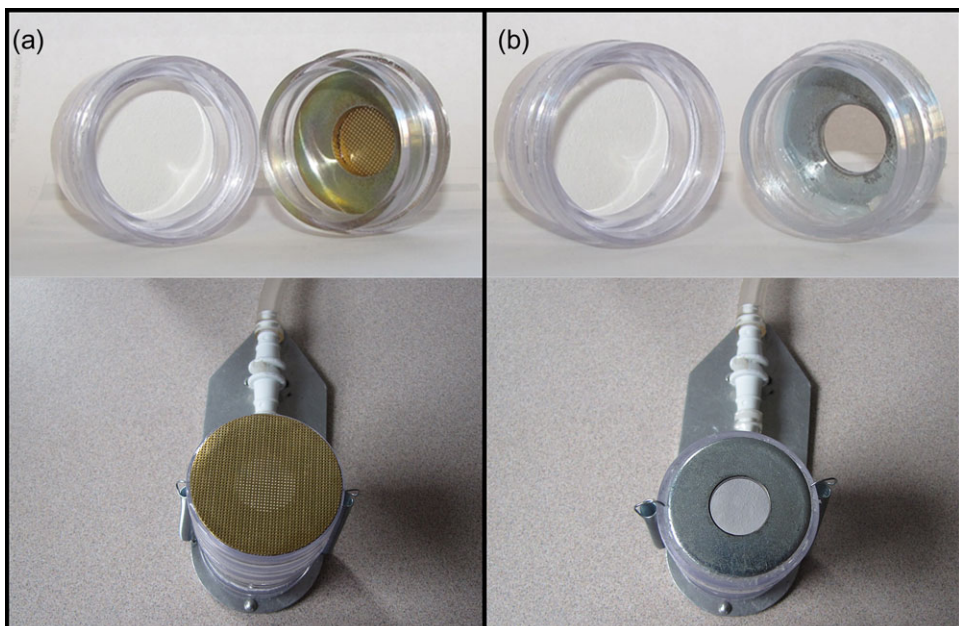


Fig. 1. (a) Photograph of constructed screened PHISH; (b) photograph of open-faced PHISH.

inlet. The latter configuration will be referred to as the open-face PHISH, which consisted of a single 15-mm diameter inlet, simply the metal washer adhered to the inner ring of a 37-mm sampling cassette, operated at 10 l min⁻¹ of flow (Fig. 1b).

This work reports facing-the-wind sampling efficiencies of three personal aerosol samplers. As only the facing-the-wind sampling efficiency was measured, comparing these results to the 'orientation-averaged' inhalability convention is inappropriate. However, results of this work may be compared to other physiologically relevant estimates of human aspiration, such as the aspiration efficiency of a mouth-breathing mannequin when facing-the-wind, as reported by Kennedy and Hinds (2002). Our wind tunnel velocity (0.4 m s⁻¹) matched the lowest wind speed tested by Kennedy and Hinds. One significant limitation, however, is that Kennedy and Hinds only determined the mannequin aspiration efficiency with solid particles. Here, we are interested in determining if differences in sampling efficiencies for personal samplers exist between solid and liquid particles. Since an estimate of facing-the-wind human (or mannequin) aspiration is not available for liquid particles, our results are only compared to the mannequin aspiration efficiency for solid particles reported by Kennedy and Hinds (2002), hereafter referred to as 'mannequin aspiration efficiency'. As such, deviations of personal sampler sampling efficiency from the Kennedy and Hinds dataset for liquid particles do not necessarily represent a deviation from physiological relevance.

METHODS

The objective of this study was to examine the sampling efficiency of the screened and open-faced PHISH inlets and two other inhalable aerosol samplers, as a function of particle size and phase (solid versus liquid). Tests were conducted in a low-velocity wind tunnel (0.4 m s⁻¹ freestream velocity) under facing-the-wind conditions over a wide range of diameters (10–100 µm). Wind speed in the tunnel was verified with a TSI Alnor Velometer Thermal Anemometer (TSI, St. Paul, MN, AVM440) multiple times during the course of wind tunnel testing. Sampling efficiency was determined for the IOM sampler (operated at 2 l min⁻¹; SKC, Inc.), the Button sampler (operated at 4 l min⁻¹; SKC, Inc.), and the prototype PHISH inlets attached to the standard open-face 37-mm cassette (operated at 10 l min⁻¹; Pall Corp., Port Washington, NY, USA).

All experiments were conducted in a horizontal wind tunnel (1 × 1 m in cross section, 3.5 m length). Air entering the tunnel was first drawn through

HEPA filters using a 3.73-kW backward curved airfoil fan. Air velocity through the tunnel was maintained at 0.4 m s⁻¹. A second set of HEPA filters, located at the rear of the tunnel, removed all test particles prior to reaching the fan and exhaust. Particles were injected into the tunnel through an opening in the ceiling, located either 0.5 m downstream of the tunnel entrance for particles with diameters <25 µm or 1.0 m downstream of the tunnel entrance for particles >25 µm, to accommodate gravitational settling of these particles in the slow-moving air.

In many wind tunnel studies, samplers are mounted on a mannequin that rotates on a vertical axis to determine the orientation-averaged sampling efficiency. Instead, in this study, samplers were mounted onto a rotating bluff-body disc (RBD) in the wind tunnel, which rotates about a horizontal axis to reduce spatiotemporal variability associated with sampling supermicron aerosol in low velocity wind tunnels (Fig. 2, Koehler *et al.*, 2011). Briefly, the RBD comprised a 40-cm diameter aluminum disc with eight sampling ports positioned equidistant about its outer edge. The disc faces the wind and rotates about its central facing-wind axis. Personal and isokinetic samplers were connected to the front face of the aluminum disc. Previous work demonstrated that isokinetic samples collected on the RBD were indistinguishable, within experimental error, to those collected with a static isokinetic sampler away from the RBD, but with reduced variance among replicate samples (Koehler *et al.*, 2011). Flow through each sampling port was regulated by a needle valve mounted on the back of the RBD. The manifold was connected to an aluminum tube that served simultaneously as the axis of rotation (horizontal) and as a conduit for airflow. A chain and sprocket assembly connected the RBD tube to a gear motor. The RBD was rotated on a horizontal axis at 2–2.5 r.p.m., resulting in 60–75 revolutions of the four sets of paired samplers around the central cross section of the wind tunnel over a typical 30 min test. As such,

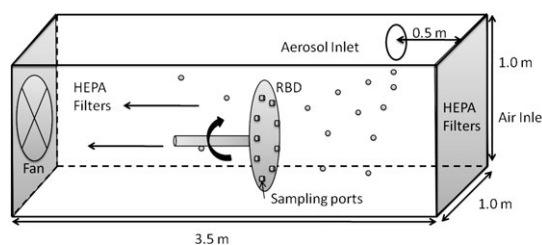


Fig. 2. Schematic of the wind tunnel showing aerosol inlet and location of the RBD.

each sampler traversed an identical path about the wind tunnel cross section, which reduced the effects of spatial heterogeneity associated with dispersing supermicron aerosol in low velocity wind tunnels. All tests were performed with the samplers facing-the-wind (0° orientation). The RBD provided a simple bluff body intended to give representative results for testing personal samplers in facing-wind orientation (Koehler *et al.*, 2011).

Liquid test particles

Monodisperse liquid test particles of ~ 10 , 30, 50, and $100\text{ }\mu\text{m}$ aerodynamic diameter were generated using a Vibrating Orifice Aerosol Generator (VOAG, model #3450; TSI Inc., Shoreview, MN, USA) and an oleic acid solution containing ammonium fluorescein. Particle diameter was verified with optical microscopy and was found to vary by $\pm 15\%$ (average coefficient of variation among measured particles of a given size) from the nominally selected size. The size of the impacted liquid droplets was determined using the experimental spread factor of oleic acid on glass (collected diameter/aerosolized diameter = 2.38, Liu *et al.*, 1982). At least three sampling efficiency tests (two replicates per test) were completed at each particle size. Although care was taken to replicate experimental duration and aerosol generation conditions among separate tests, the between-test aerosol concentrations were highly variable. However, despite the differences in aerosol mass concentrations, filter loadings never approached saturation and sampler flow remained constant over each testing cycle.

When sampling liquid particles, the isokinetic probes were made of stainless steel tubing (0.95 cm outer diameter, 0.67 cm inner diameter), each with a beveled edge leading into the flow. Probe inlets were attached to standard two-piece 37-mm filter cassettes (Millipore Inc., Billerica, MA, USA) by drilling out the inlet cap and using epoxy to seal the isokinetic inlet to the cap. Flow through each isokinetic inlet was set at 0.871 min^{-1} to match the probe sampling velocity with the wind tunnel freestream velocity (0.4 m s^{-1}). Two isokinetic samplers were mounted on the RBD for each liquid aerosol test.

For measurements of fluorescently labeled particles, collected mass was extracted and then quantified by excitation–emission spectroscopy. Deposition on both the filter media and internal sampler components were examined to quantify internal surface losses associated with each sampler. For the isokinetic samplers, filter substrates and isokinetic sampler inlets were placed in separate 15-ml centrifuge tubes and extracted with 4 ml of 3% ammonium hydroxide solution. The outside of the isokinetic sampler inlets was

cleaned with an alcohol-wetted wipe to remove any particles that deposited on the outer surface of the inlet prior to extraction. The isokinetic probe was inset far into the cassette such that losses to the cassette wall were minimized. Therefore, the cassette walls surrounding the isokinetic probe were not wiped for analysis.

The IOM inlet and filter were also placed in separate centrifuge tubes and extracted with 8 and 4 ml of ammonium hydroxide solution, respectively. The Button inlet (screened cap) and filter were extracted separately and in similar fashion to the IOM procedure. The outer non-perforated edge of the Button inlet was wrapped with Teflon tape during sampling and was removed prior to extraction so that particles depositing on the inlet edges (outside of the screen face) would not contribute to the fluorescent mass detected (i.e. only particles that collected on the screen portion of the Button sampler were quantified to assess particle losses during aspiration). Particle deposition onto the O-rings for either the IOM or Button were not assessed. The PHISH screen (when applicable) and filter were extracted in separate 4 ml solutions; a cotton swab was used to wipe the inside of the PHISH and 37-mm cassette spacer and this swab was then placed in a separate centrifuge tube with 4 ml of extraction solution to assess particle losses between the inlet and the filter.

All solutions were sonicated for 10 min to ensure efficient extraction. Three aliquots of 200 μl (i.e. triplicate samples) were pipetted into 96-well plates and analyzed in a fluorescence plate reader (FLX-800; BioTek Inc., Winooski, VT, USA). Results are reported in relative fluorescence units (RFU), which is a reliable surrogate for mass. Serial dilutions of calibration standards were analyzed to ensure linearity of the fluorescence signal over the range of concentrations sampled. The limit of quantification for the fluorescence measurements was 10 RFU, corresponding to $\sim 0.5\text{ ng}$ of fluorescein per sample; data from an experiment were used only if all measured values on the filters were above this limit.

Solid test particles

Two methods were required to generate monodisperse, solid test particles. Fluorescein-labeled NaCl particles of $13\text{ }\mu\text{m}$ diameter were generated with the VOAG and extracted for analysis as described above. For larger particle diameters, the VOAG produced very large ($>100\text{ }\mu\text{m}$) hollow spheres upon drying instead of compact spheres of the correct diameter, when examined by microscopy. This phenomenon can be eliminated by slowing the drying time of generated droplets (Leong, 1981; Cheng

et al., 1988), however, our experimental setup precluded the use of such a drying column. Instead, oxidized alumina powder (Duralum, Washington Mills, North Grafton, MA, USA) was dispersed using a Wright-type dust feeder with median aerodynamic diameters of 33, 66, and 94 μm . Solid particle diameters were verified with optical microscopy and found to vary by $\sim 30\%$ from the nominally selected size.

Aerosol concentration was determined by gravimetry for the alumina particle tests. All samples were collected on Teflon-coated glass fiber filters (Pallflex Fiberfilm #T60A20). The cassettes and filters were stored in a low relative humidity equilibration chamber for at least 12 h before obtaining pre- and post-sampling weights and were neutralized on a Polonium²¹⁰ strip for at least 15 s prior to weighing. A Mettler-Toledo MX5 analytical microbalance (Columbus, OH, USA), accurate to $\pm 1\ \mu\text{g}$, was used to obtain all weights. The mass of alumina collected was generally between 100 and 1000 μg . All mass measurements exceeded our analytic limit of quantification for gravimetric analysis, defined as 10 times the standard deviation of repeated blank weights taken across multiple days. The limit of quantification was 112 μg for the Button sampler (for the combined filter and *o*-ring weight, see below), 250 μg for the IOM sampler, and 260 μg for the PHISH sampler (using the modified ACCU-CAP, see below). Field blanks were included for each day and used to correct the mass measured on each sampling filter.

For the solid particle tests, the isokinetic sampler was adjusted to accommodate greater mass capture for gravimetric analysis. These isokinetic probes (12.7 mm outer diameter, 10.2 mm inner diameter) were sealed into the inlet of a stainless steel IOM and operated at 1.96 $1\ \text{min}^{-1}$ to accommodate the larger mass needs. After sampling, the inside of the isokinetic inlets were rinsed with ethanol and the elution was captured onto a separate 37-mm filter. This filter was left to dry in a desiccating chamber for at least 12 h and then weighed separately from the isokinetic sampler filter.

When the Button sampler was challenged with solid particles larger than $\sim 30\ \mu\text{m}$, a visible layer of dust was observed on the inner edge of the Teflon *o*-ring used to seal the filter cassette assembly. Therefore, both the filter and *o*-ring were weighed together for both the pre- and post-weight. This is likely the result of particle migration from the filter to the *o*-ring because of the rotation and vibration of the RBD during use. While liquid particles were effectively retained within the filter matrix, large solid particles appeared to migrate to the internal walls of the

sampler. This also proved to be a problem for the open-faced PHISH; a large portion of the sample appeared to migrate to the edges of the 37-mm cassette. To prevent such internal wall losses, ACCU-CAP filters (SKC, Inc.) were modified to retain the alumina samples. The ACCU-CAP bubble was removed from its original filter and enlarged to 25 mm using a stainless steel punch. The modified ACCU-CAPs were then glued to sheets of the filter material, allowed to dry, and then punched to create a 37-mm diameter filter attached to a 25 mm ACCU-CAP inlet. After gluing, the modified ACCU-CAPs were baked at 50°C overnight then stored in a desiccator for at least 48 h prior to use. Tests were not performed with the screened PHISH with solid particles due to poor performance of the screened PHISH sampling droplets (see PHISH: Screened and Open-Faced). No modifications were made to IOM cassette or weighing procedure as the entire IOM cassette and filter are designed to be weighed together to preclude bias from wall losses during gravimetric analysis.

Estimating sampling efficiency and losses

As defined in the Introduction, the aspiration efficiency is the efficiency with which particles are transported from the ambient air into the inlet of a sampler (Paik and Vincent, 2004). This is in contrast to the sampling efficiency, the efficiency with which particles are transported to the collection substrate for quantification. Of the samplers examined here, the aspiration efficiency is equal to the sampling efficiency only for the IOM since the IOM inlet is designed to be a part of the collection substrate. The sampling efficiency is less than the aspiration efficiency for the Button and PHISH samplers due to transmission losses. The sampling efficiency was computed as the ratio of the aerosol concentration measured by a sampler (the entire IOM cassette or the filters only for the Button and PHISH samplers) compared to the average aerosol concentration measured by two sharp-edged isokinetic probes (collocated with the given sampler during each test). For each sampler, sampling efficiencies were compared between particle type (liquid versus solid) and at each particle size using unpaired *t*-tests.

Sampling efficiencies were also compared to published values for facing-the-wind mannequin aspiration efficiency at 0.4 m s^{-1} freestream condition (Kennedy and Hinds, 2002, see below). A comparison to the orientation-averaged inhalability criterion is not appropriate here, as only facing-the-wind sampling efficiency was evaluated. The root mean square error (RMSE) was computed as the square root of the

squared difference between the observed sampling efficiency of the sampler and the facing-the-wind mannequin aspiration efficiency at 0.4 m s^{-1} for each diameter, summed over all measured diameters. Smaller RMSE values indicate improved agreement with the published data on mannequin aspiration efficiency when facing the wind.

Finally, the use of fluorescently labeled aerosol allowed for estimation of droplet mass depositing to various regions (inlet, inner cassette walls, or filter) of each sampler. As such, we assessed particle losses onto and within the sampler during aspiration and transmission. The sum of these regional collection efficiencies, when combined with the sampling efficiency, provides an estimate of the aspiration efficiency for a given sampler. Losses to the screen and internal walls of the Button sampler were estimated by extracting the screen and wiping the internal sampler walls, respectively. Transmission losses within the PHISH sampler were estimated from a wipe of the inner surfaces of the PHISH cassette. The filter and inlet cassette of the IOM sampler were analyzed separately to determine the proportion of particle mass that did not reach the filter, even though these pieces are typically analyzed together.

RESULTS AND DISCUSSION

To validate our experimental setup, we first determined the sampling efficiency of the three personal samplers with $\sim 1 \mu\text{m}$ fluorescent liquid aerosol. We expected that the sampling efficiency at this size would be $\sim 100\%$ for all sampler types. We observed sampling efficiencies of 105, 94, and 96% for the Button, IOM, and PHISH, respectively (data not shown) and these sampling efficiencies were not significantly different from each other.

Sampling efficiency

Measured sampling efficiencies of the IOM, Button, and open-faced PHISH personal samplers are presented in Figs 3–5, respectively. Each data point represents the average of at least six replicates (three tests, two duplicate samplers per test). Error bars represent 1 SD, which was estimated by propagation of errors for both the test and reference (isokinetic) samplers. We have grouped the $13 \mu\text{m}$ diameter solid particles and $10 \mu\text{m}$ diameter liquid particles into a single $\sim 10 \mu\text{m}$ size range to simplify the discussion that follows. Similarly, we grouped the Alumina particle sizes with the similarly sized droplets into ~ 30 , ~ 50 , and $\sim 100 \mu\text{m}$ size ranges. In each figure, the mannequin aspiration efficiency at a wind speed of 0.4 m s^{-1} reported by Kennedy and Hinds (2002)

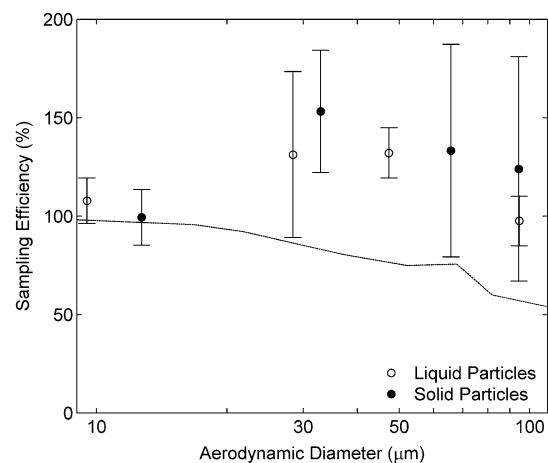


Fig. 3. Facing-the-wind sampling efficiency for the IOM sampler as a function of particle size and phase. Filled symbols represent solid particles and open symbols represent liquid particles. Facing-the-wind mannequin aspiration efficiency at 0.4 m s^{-1} is shown as a solid line, for comparison (Kennedy and Hinds, 2002).

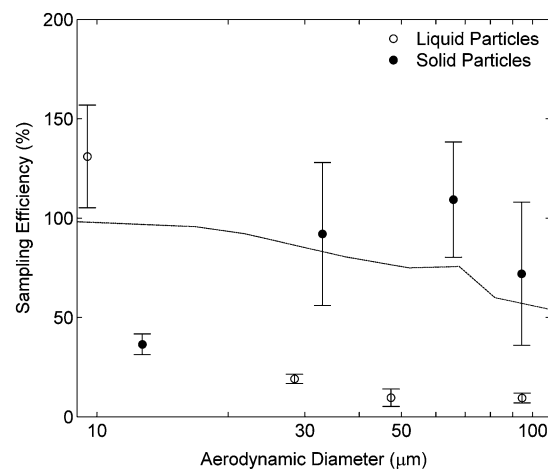


Fig. 4. Facing-the-wind sampling efficiency for the Button sampler as a function of particle size and phase. Filled symbols represent solid particles and open symbols represent liquid particles. Facing-the-wind mannequin aspiration efficiency at 0.4 m s^{-1} is shown as a solid line, for comparison (Kennedy and Hinds, 2002).

is shown as a solid black line for comparison. The RMSE values for both solid and liquid particles are provided in Table 1.

IOM sampler. Sampling efficiency of the IOM sampler challenged with solid and liquid particles is shown in Fig. 3. For all sizes and both particle types, the IOM overestimated the facing-the-wind mannequin aspiration efficiency. This result has been

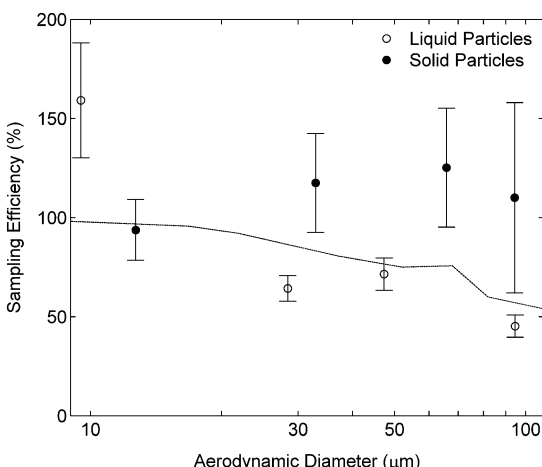


Fig. 5. Facing-the-wind sampling efficiency for the open-faced PHISH as a function of particle size and phase. Filled symbols represent solid particles and open symbols represent liquid particles. Facing-the-wind mannequin aspiration efficiency at 0.4 m s^{-1} is shown as a solid line, for comparison (Kennedy and Hinds, 2002).

Table 1. RMSE values ± 1 SD between measured aspiration and published values of facing-the-wind mannequin aspiration efficiency for samplers challenged with solid and liquid particles.

Sampler	Solid	Liquid
IOM	1.12 ± 0.22	0.84 ± 0.17
Button	0.72 ± 0.17	1.10 ± 0.17
PHISH (open-faced)	0.80 ± 0.17	0.66 ± 0.17

observed by other researchers for both solid (Li *et al.*, 2000) and liquid (Zhou and Cheng, 2010) particles at somewhat higher wind velocity (0.55 m s^{-1}). Differences in IOM sampling efficiency between solid and liquid particles were not statistically different for any size (unpaired *t*-test, $0.07 < P < 0.82$). The coefficient of variation for replicate samplers was $<20\%$ for diameters $<100 \mu\text{m}$ and between 30 and 40% for the $\sim 100 \mu\text{m}$ particle size. Due primarily to the better agreement with the facing-the-wind sampling efficiency at diameters $\sim 50 \mu\text{m}$ and larger, the RMSE for the liquid aerosol was smaller than for the solid aerosol.

Facing-the-wind sampling efficiencies for the IOM at a wind speed of 0.55 m s^{-1} reported by Li *et al.* (2000) for solid particles were in good agreement with those found in this study, despite the $\sim 25\%$ lower wind speed used here. Zhou and Cheng (2010) found generally lower sampling efficiency for liquid particles, particularly for particle diameters between ~ 30 and $\sim 50 \mu\text{m}$. Roger *et al.* (1998) also

reported facing-the-wind sampling efficiencies for 1 and 3 m s^{-1} wind speeds. Their results indicated higher sampling efficiencies than found here for either the solid or liquid particles, likely due to the increased wind speed. The facing-the-wind sampling efficiency of the IOM has a well-known dependence with increasing wind speed (Roger *et al.*, 1998; Li *et al.*, 2000).

Button sampler Sampling efficiencies of the Button sampler were significantly different between solid and liquid particles for all sizes ($P < 0.0002$, Fig. 4). For solid particles $\sim 30 \mu\text{m}$ and larger, the Button sampler showed better agreement to the mannequin aspiration efficiency than the IOM (RMSE 65% of that for the IOM) yet still had a tendency to oversample. However, when challenged with droplets, the sampling efficiency of the Button sampler reduced to $<20\%$ for particles $\sim 30 \mu\text{m}$ and larger resulting in a much larger RMSE than observed for the IOM. The coefficient of variation for replicate Button samplers was generally less than 35%.

The sampling efficiency measured for $\sim 10 \mu\text{m}$ solid particles was much $<100\%$. It is unclear why the discrepancy between the solid and liquid particles was observed at this size. Although droplets do not bounce upon impactation with the screened inlet, large solid particles likely bounce and were ultimately aspirated. However, for solid particles $\sim 10 \mu\text{m}$ in diameter, it is unclear how these particles behave as they approach the Button sampler's screened inlet. For low wind speeds in the tunnel, like those used here, these particles may not have sufficient kinetic energy to bounce off the inlet screen. Xu and Willeke (1993) modeled the threshold size for aerosol bounce as a function of particle composition, surface material, and the velocity of the approaching aerosol. They estimated that $7 \mu\text{m}$ ammonium fluorescein particles would bounce off surfaces only for approaching velocities exceeding $0.7\text{--}1.1 \text{ m s}^{-1}$, depending on the surface material. For smaller particles or lower wind velocities, particles will not bounce. Although the $\sim 10 \mu\text{m}$ NaCl particles tested here are of different composition than those modeled by Xu and Willeke, the low wind speed in the tunnel (0.4 m s^{-1}) and nominal airspeed at the sampler pores (0.2 m s^{-1}) suggests that bounce may not occur for this size range. Small differences in aerodynamic diameter and wind speed in the tunnel may have resulted in the discrepancy in sampling efficiency observed for the solid and liquid $\sim 10 \mu\text{m}$ particles.

Initial studies with the Button sampler employed the unit at 2 l min^{-1} of flow (Kalatoor *et al.*, 1995; Li *et al.*, 2000). However, aspiration models

developed by Gao *et al.* (2002) suggested that a flow of 2 l min^{-1} resulted in non-uniform velocity vectors at the edges of the screened inlet (causing aspirated particles to flow back out of the sampler). Consequently, Gao *et al.* recommended a higher flow rate. More recent studies of orientation-averaged sampling efficiency (Aizenberg *et al.*, 2000; Aizenberg *et al.*, 2001; Witschger *et al.*, 2004; Gorner *et al.*, 2010) have employed the Button sampler at 4 l min^{-1} to reduce this effect. Although some experimental studies have suggested that facing-the-wind aspiration for $10\text{ }\mu\text{m}$ particles should be near 100% (Li *et al.*, 2000, at 2 l min^{-1}), other experimental and modeling studies have suggested lower facing-the-wind sampling efficiencies at both sampler flow rates for $10\text{ }\mu\text{m}$ sized solid particles (Aizenberg *et al.*, 2000; Kalatoor *et al.*, 1995; Gao *et al.*, 2002), in better agreement with our observations. Modeling studies of droplet aspiration are in good agreement with our observations (Gao *et al.*, 2002).

PHISH: screened and open-faced. As with the Button sampler, the screened inlet of the PHISH greatly impeded droplet aspiration. Measured sampling efficiencies, as determined from the mass collected on the filter only, for liquid particles between 10 and $100\text{ }\mu\text{m}$ were $<20\%$ (data not shown), in good agreement with modeled values (Anthony *et al.*, 2010). Therefore, sampling efficiency was also determined for an open-faced PHISH (the same flat-faced sampler but with the screened inlet replaced with a single 15-mm circular opening—shown in Fig. 1b). Measured sampling efficiency for the open-faced PHISH (Fig. 5) showed reasonable agreement with the mannequin aspiration efficiency, with solid particles being somewhat oversampled and liquid particles being somewhat under-sampled (all sizes except $\sim 10\text{ }\mu\text{m}$). Although the difference in sampling efficiency between the solid and liquid particles was not as pronounced for the open-faced PHISH as for the Button sampler, sampling efficiencies for solid particles were significantly larger than for the liquid particles ($\geq 30\text{ }\mu\text{m}$, $P < 0.007$). However, for the smallest size, the sampling efficiency of liquid particles was significantly larger than for the solid particles ($P = 0.0001$). Yet the open-faced PHISH, operating under facing-the-wind conditions had the smallest RMSE for liquid particles compared to the other two personal samplers and RMSE between the Button sampler and IOM sampler for solid particles. The coefficient of variation for replicate samplers was generally $<15\%$.

The open-inlet PHISH is similar in construction to a modified 37-mm cassette (Mod37) as proposed by Clinkenbeard *et al.* (2002), which had a 15 mm

circular diameter orifice with a thin lip that protruded outward and operated 0° down orientation (parallel to the floor) at 2 l min^{-1} of flow. The PHISH (screened or open-faced) does not have such a lip. Clinkenbeard *et al.* (2002) found that the wiped Mod37 oversampled relative to the IOM for field sampling of sanding and spraying operations. The difference in flow rate, wind speed, and the forward-facing directionality may explain the better agreement with mannequin aspiration efficiency for the open-faced PHISH than observed for the Mod37. The open-faced PHISH and Button samplers showed very similar sampling efficiencies for solid particles, but the open-faced PHISH showed better agreement with the facing-the-wind mannequin aspiration efficiency when sampling liquid particles. The open-faced PHISH also showed better agreement with the mannequin aspiration efficiency than was reported for a standard closed-face 37-mm cassette for solid particles at a wind speed of 0.55 m s^{-1} (Li *et al.*, 2000).

Losses during aspiration and transmission

As mentioned in Methods, fluorescently tagged solid particles could not be generated with the VOAG for diameters larger than $\sim 30\text{ }\mu\text{m}$ because large particles required extensive drying times at high relative humidity to result in compact solid particles (Leong, 1981; Cheng *et al.*, 1988). This could not be accommodated with our wind tunnel geometry. As such, estimates of solid particle deposition to various sampler regions were only available for the smallest size range ($\sim 10\text{ }\mu\text{m}$). For the Button and the open-faced PHISH, particles depositing onto the inlet and inner cassette walls would not be included in a sample analysis where only the filter is weighed. Alternatively, with the IOM, the inlet portion of the cassette is typically weighed with the filter so that particles depositing onto both the filter and inlet contribute to a typical gravimetric analysis (a particularly innovative design aspect that is unique to the IOM).

A comparison of the solid and liquid sampling efficiencies plus the collection efficiency of particle losses during aspiration and transmission, where available, are shown for each sampler in Figs 6–8. For solid particles, regional mass deposition was not assessed $>10\text{ }\mu\text{m}$, and only the sampling efficiency measured by the filter (Button and open-faced PHISH) or filter and inlet/cassette (IOM), defined as the estimated concentration from the filter or filter and inlet/cassette divided by the concentration estimated by the sharp-edged isokinetic sampler, are presented (black bars). For the fluorescently labeled

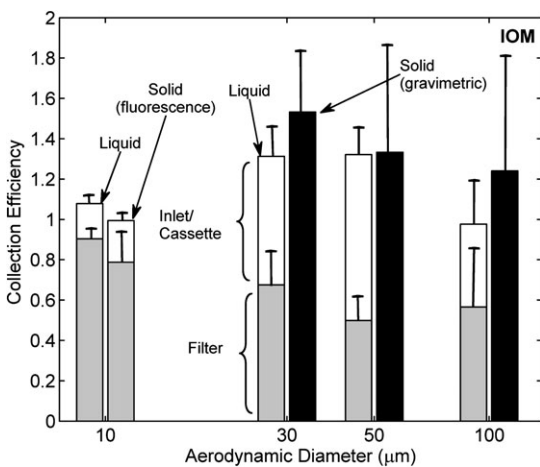


Fig. 6. IOM fractional collection efficiency defined as the concentration measured on each sampler component relative to the concentration measured by a sharp-edged isokinetic sampler as a function of particle size and type (solid particles versus droplets) at 0.4 m s^{-1} wind speed. Black bars represent fractional collection efficiency for solid particles by gravimetry (i.e. the sampling efficiency). Gray bars represent the collection efficiency of the filter; white bars depict the collection efficiency of the sampler inlet/cassette as determined by fluorescence analysis.

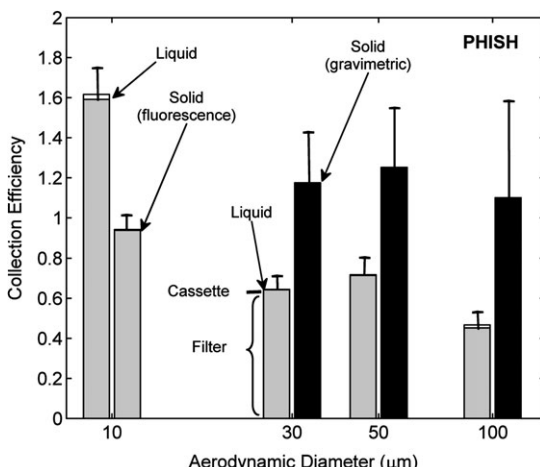


Fig. 8. Open-faced PHISH fractional collection efficiency defined as the concentration measured on each sampler component relative to the concentration measured by a sharp-edged isokinetic sampler as a function of particle size and type (solid particles versus droplets) at 0.4 m s^{-1} wind speed. Black bars represent fractional collection efficiency for solid particles by gravimetry (i.e. the sampling efficiency). Gray bars represent the collection efficiency of the filter (i.e. the sampling efficiency); white bars depict the collection efficiency of the cassette estimated by wiping the inside of the open-faced PHISH and cassette as determined by fluorescence analysis.

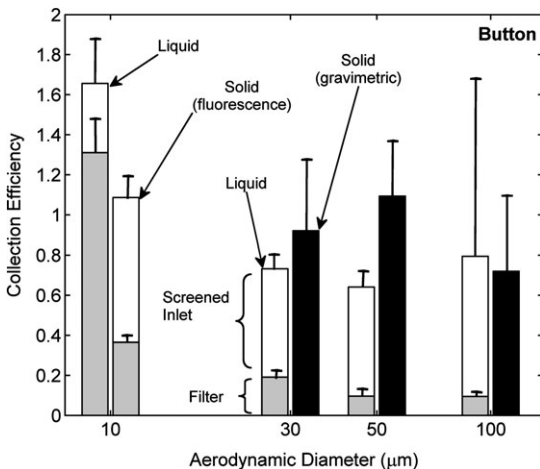


Fig. 7. Button fractional collection efficiency defined as the concentration measured on each sampler component relative to the concentration measured by a sharp-edged isokinetic sampler as a function of particle size and type (solid particles versus droplets) at 0.4 m s^{-1} wind speed. Black bars represent collection efficiency for solid particles by gravimetry (i.e. the sampling efficiency). Gray bars represent the collection efficiency of the filter (i.e. the sampling efficiency); white bars depict the collection efficiency of the sampler's screened inlet as determined by fluorescence analysis.

particles, the sampling efficiency of particles deposited on each sampler's filter (gray bars) and the regional collection efficiency (white bars), either

onto the meshed inlet (Button) or onto the inner surfaces of the filter cassette (IOM, open-faced PHISH) are summed to estimate the aspiration efficiency as defined earlier. For the Button sampler, this may yield an overestimation of aspiration efficiency since both sides of the screen are extracted together and particles depositing on the front of the screen are not truly aspirated. Error bars represent 1 SD of efficiency for each component presented. Only positive error bars are shown for clarity.

IOM sampler. The sampling efficiencies for droplet experiments are presented in the left bars and solid particle experiments are shown in the right bars in Fig. 6, as a function of aerodynamic particle diameter. For the IOM, the white bars represent the collection efficiency of the inlet/cassette.

Roughly 26–62% of the droplets entering the IOM were deposited on the walls of the inlet/cassette assembly. However, such transmission losses do not pose a sampling problem for gravimetric analysis using IOM samplers, since the entire cartridge is intended to be weighed. However, for other types of physicochemical analyses, care must be taken during analysis since a portion of the aspirated aerosol does not reach the filter. In the UK, the Health and Safety Executive Methods of Determination of Hazardous

Substances typically call for cassette extraction where the material on the cassette is intended to be a part of the sample, as is the case for the IOM sampler (e.g. HSE, 1998, 2006). However, in the USA, as noted by Harper and Demange (2007), many Occupational Safety and Health Administration (OSHA) and NIOSH Methods do not explicitly detail how inlet losses or internal cassette deposits should be treated. Our results confirm the need for analyzing inlet/cassette deposits when sampling inhalable aerosols. At $\sim 10 \mu\text{m}$, transmission losses were similar between solid and liquid particles. Above $10 \mu\text{m}$, we determined transmission losses only for liquid particles. Kenny *et al.* (1997) reported that inlet/cassette losses for solid particles were size dependent and up to 25% for $\sim 100 \mu\text{m}$ particles. However, other studies have indicated inlet/cassette losses in better agreement with the droplet losses reported here. Witschger *et al.* (2004) observed inlet/cassette losses of 20% for $6.9 \mu\text{m}$ solid particles up to 55% for $76 \mu\text{m}$ solid particles. Additionally, Mark (1990) suggested inlet/cassette losses between 25 and 44% for solid particles between 6 and $34 \mu\text{m}$.

Button sampler. The collection efficiencies for the different Button sampler components are shown in Fig. 7, where the white bars represent the collection efficiency of the screened inlet, as determined by fluorescence analysis. The diminished droplet sampling efficiency for the Button sampler, when analyzing the filter only, is due to losses at the screened inlet. For $\sim 100 \mu\text{m}$ droplets, seven times more mass was deposited on the screen than on the filter. If one were to extract the deposited mass on the screen and filter together, reasonable agreement with the mannequin aspiration efficiency could be obtained. However, the screen is too heavy for gravimetric analysis, so this is only feasible if deposited particles can be removed with a wash-off method, as was done here. Thus, we recommend that a personal sampler with a non-meshed surface be used if droplet exposures are to be assessed. Since sampling efficiencies are in better agreement with the mannequin aspiration efficiency for the larger solid particles ($\geq 30 \mu\text{m}$), we assume that the solid particles indeed bounce and fewer particles deposit on the inlet screen. Our results suggest that the Button performance is generally acceptable for assessing exposures to solid particles. However, the issue of bounce for solid particles with diameter $\sim 10 \mu\text{m}$ and smaller should be investigated further for this sampler.

PHISH: open-faced. The collection efficiencies of particles depositing on the different components of the open-faced PHISH are shown in Fig. 8, where

the white bars represent the collection efficiency estimated by the wipe of the inner cassette surfaces, determined by fluorescence analysis.

Negligible transmission losses were observed for the open-faced PHISH challenged with droplets and $\sim 10 \mu\text{m}$ solid aerosol (relative mass on wipe $<2\%$ of relative mass on filter). Only error bars on the collection efficiency of the filter are visible in this figure. The negligible transmission losses suggest that the discrepancy in sampling efficiency between solid and liquid particles $\sim 30 \mu\text{m}$ and larger is due to particle bounce on the exterior surface of the sampler. Solid particles likely bounce off the open-faced PHISH face and are ultimately aspirated, while liquid particles do not bounce and the aspiration efficiency is reduced. The reduced sampling efficiency of $\sim 10 \mu\text{m}$ solid particles compared to $\sim 10 \mu\text{m}$ droplets is unclear and the influence of particle bounce at small diameters should be investigated further.

Clinkenbeard *et al.* (2002) found that wall losses inside the Mod37 were substantial and that analysis of the filter alone (without accounting for losses by wiping the internal cassette walls) would likely result in underestimation of exposure. However, in their study, the swabs and filters were analyzed together, thus the percentage of mass depositing in each of these regions is uncertain. In addition, the difference in flow rate between the Mod37 (2 l min^{-1}) and the open-faced PHISH sampler (10 l min^{-1}) may account for different regional deposition within the sampler as the larger flow rate may reduce wall losses by reducing particle residence time inside the cassette. Although the transmission losses for the alumina aerosol were not measured, we found that a modified ACCU-CAP was necessary to recover solid particles sampled by the open-faced PHISH. Gorner *et al.* (2010) also found that the ACCU-CAP could improve orientation-averaged sampling efficiency for a standard closed-face 37-mm cassette. Puskar *et al.* (1991) found that when closed-face two-piece cassettes sampled pharmaceutical dusts, only 22% of the mass deposited on the filter, while 62% of the dust mass was on the inside surface of the cassette top, and the remaining 16% was on the interior walls of the cassette. They deduced that electrostatic attraction during sampling and/or shipping and handling of the cassettes led to the large portion of sample on the cassette top and that the small portion on the cassette bottom was the result of losses during cassette handling. Since the PHISH samplers were mounted on a rotating surface (RBD), the problem of solid particles migrating to the edge of the filter was likely exacerbated in our experiments. However, particles are probably disturbed inside these samplers during personal exposure

assessments in the field as well, due to actions by the wearer. Differences between these actions cannot be assessed here. However, our results suggest that 37-mm cassettes using the open-faced PHISH inlet may provide a reasonable match to the facing-the-wind mannequin aspiration efficiency, but that the inner cassette 'should be wiped' before analysis, in agreement with the OSHA perspective for metals analysis (Hendricks *et al.*, 2009). Alternatively, use of a modified ACCU-CAP to fit this new sampler might retain the advantages of the classic 37-mm cassette, while improving sample mass capture and agreement with the mannequin aspiration efficiency.

Additionally, Zhou and Cheng (2010) measured the droplet sampling efficiency of the IOM at a larger flow rate than is currently specified (10.6 l min⁻¹) and a wind speed of 0.56 m s⁻¹. Those authors found lower sampling efficiencies for ~10 µm droplets and higher sampling efficiency for larger particles than observed here for the open-faced PHISH. Although the open-faced PHISH here and the IOM in that study both operated at ~10 l min⁻¹ and had an identical inlet size, these differences may be due to differences in inlet geometry (i.e. the PHISH does not have a protruding lip as does the IOM) and in wind speed (0.4 m s⁻¹ here and 0.56 m s⁻¹ in that study).

CONCLUSIONS AND STUDY LIMITATIONS

The facing-the-wind sampling efficiency of three personal aerosol samplers was investigated at a wind speed of 0.4 m s⁻¹ for both solid and liquid particles. Four major conclusions can be drawn from this work. (1) Screened samplers aspirate large droplets with significantly reduced efficiency as compared to solid particles. Consequently, open-inlet samplers should be used when assessing exposures to droplets. (2) Measurements of aspiration losses suggest that solid particles bounce off the surface of screened samplers allowing them to be re-entrained into the airstream and ultimately aspirated into the sampler. This finding corroborates fluid dynamics modeling showing that bounce is an important factor during particle aspiration (Anthony *et al.*, 2010). (3) The open-faced PHISH showed the best agreement to the facing-the-wind mannequin aspiration efficiency at 0.4 m s⁻¹ wind speed for liquid particles, when compared to the IOM and Button sampler. This design also offers cost advantages over the IOM and Button samplers. (4) The extent of solid particle bounce likely diminishes as particle size decreases (approaching ~10 µm under conditions tested here). Furthermore, our understanding of particle bounce is somewhat limited.

While a large amount of information on particle bounce inside ducts is available (e.g. Peters and Leith, 2004a,b), additional theoretical and experimental work is needed, to describe and quantify this phenomenon on the exterior surfaces of personal samplers under realistic (i.e. workplace) conditions.

Many limitations inherent to this study suggest avenues for continued research. This work did not evaluate orientation-averaged sampling efficiency for any of the personal aerosol samplers, although the work was compared to measured estimates of human aspiration (mannequin aspiration efficiency) in matched experimental conditions. This work evaluated only one wind speed (0.4 m s⁻¹) and samplers are likely to perform differently as the freestream velocity is further decreased. In addition, regional losses for solid particles larger than ~10 µm were not evaluated. Future work should also determine whether an AccuCap could be adapted to the PHISH.

FUNDING

National Institute for Occupational Safety and Health (R21OH009114).

REFERENCES

- ACGIH. (1999) Particle size-selective sampling for particulate air contaminants. Cincinnati, OH: American Conference of Governmental Industrial Hygienists.
- ACGIH. (2006) 2006 TLVs and BEIs. Threshold limit values for chemical substances and physical agents. Cincinnati, OH: American Conference of Governmental Industrial Hygienists.
- Aizenberg V, Choe K, Grinshpun SA *et al.* (2001) Evaluation of personal aerosol samplers challenged with large particles. *J Aerosol Sci*; 32: 779–93.
- Aizenberg V, Grinshpun SA, Willeke K *et al.* (2000) Performance characteristics of the button personal inhalable aerosol sampler. *AIHAJ*; 61: 398–404.
- Amin MK, Womac AR, Bui QD *et al.* (1999) Air sampling of aerosol and gaseous pesticides. *Trans ASAE*; 42: 593–600.
- Anthony TR, Landazuri AC, Van Dyke M *et al.* (2010) Design and computational fluid dynamics investigation of a personal, high flow inhalable sampler. *Ann Occup Hyg*; 54: 427–42.
- Beaulieu HJ, Fidino AV, Kim L *et al.* (1980) A comparison of aerosol sampling techniques: "open" versus "closed-face" filter cassettes. *AIHAJ*; 41: 758–65.
- Buchan RM, Soderholm SC, Tillery MI. (1986) Aerosol sampling efficiency of 37 mm filter cassettes. *AIHAJ*; 47: 825–31.
- Carlton GN. (2003) The impact of a change to inhalable occupational exposure limits: strontium chromate exposure in the US Air force. *AIHAJ*; 64: 306–11.
- Cheng RJ, Blanchard DC, Cipriano RJ. (1988) The formation of hollow sea-salt particles from the evaporation of drops of seawater. *Atmos Res*; 22: 15–25.
- Clinkenbeard RE, England EC, Johnson DL *et al.* (2002) A field comparison of the IOM inhalable aerosol sampler

- and a modified 37-mm cassette. *Appl Occup Environ Hyg*; 17: 622–27.
- Gao P, Chen BT, Baron PA *et al.* (2002) A numerical study of the performance of an aerosol sampler with a curved, blunt, multi-orificed inlet. *Aerosol Sci Technol*; 36: 540–53.
- Glindmeyer HW, Lefante JJ, Rando RJ *et al.* (2004) Spray-painting and chronic airways obstruction. *Am J Ind Med*; 46: 104–11.
- Horner P, Simon X, Wrobel R *et al.* (2010) Laboratory study of selected personal inhalable aerosol samplers. *Ann Occup Hyg*; 54: 165–87.
- Harper M, Demange M. (2007) Analytical performance criteria - Concerning sampler wall deposits in the chemical analysis of airborne metals. *J Occup Environ Hyg*; 4: D81–6.
- Hendricks W, Stones F, Lillquist D. (2009) On wiping the interior walls of 37-mm closed-face cassettes: an OSHA perspective. *J Occup Environ Hyg*; 6: 732–34.
- HSE. (1998) Lead and inorganic compounds of lead in air. MDHS 6/3. London: the United Kingdom's Health and Safety Executive.
- HSE. (2006) Metals in air by ICP-MS. MDHS 99. London: The United Kingdom's Health and Safety Executive.
- IFA. (2011) GESTIS international limit values. http://www.dguv.de/ifa/en/gestis/limit_values/index.jsp. Accessed 6 October 2011.
- Kalatoor S, Grinshpun SA, Willeke K *et al.* (1995) New aerosol sampler with low wind sensitivity and good filter collection uniformity. *Atmos Environ*; 29: 1105–12.
- Kennedy NJ, Hinds WC. (2002) Inhalability of large solid particles. *J Aerosol Sci*; 33: 237–55.
- Kennedy NJ, Tatyani K, Hinds WC. (2001) Comparison of a simplified and full-size mannequin for the evaluation of inhalable sampler performance. *Aerosol Sci Technol*; 35: 564–68.
- Kenny LC, Aitken R, Chalmers C *et al.* (1997) A collaborative European study of personal inhalable aerosol sampler performance. *Ann Occup Hyg*; 41: 135–53.
- Kenny LC, Aitken RJ, Baldwin PEJ *et al.* (1999) The sampling efficiency of personal inhalable aerosol samplers in low air movement environments. *J Aerosol Sci*; 30: 627–38.
- Koehler KA, Anthony TR, Van Dyke M *et al.* (2011) A rotating, bluff-body disc for reduced variability in wind tunnel aerosol studies. *Ann Occup Hyg*; 55: 86–96.
- Leong KH. (1981) Morphology of aerosol-particles generated from the evaporation of solution drops. *J Aerosol Sci*; 12: 417–35.
- Li SN, Lundgren DA, Rovell-Rix D. (2000) Evaluation of six inhalable aerosol samplers. *AIHAJ*; 61: 506–16.
- Lillienberg L, Andersson EM, Jarvholm B *et al.* (2010) Respiratory symptoms and exposure-response relations in workers exposed to metalworking fluid aerosols. *Ann Occup Hyg*; 54: 403–11.
- Liu BYH, Pui DYH, Wang XQ. (1982) Drop size measurement of liquid aerosols. *Atmos Environ*; 16: 563–67.
- Mark D. (1990) The use of dust-collecting cassettes in dust samplers. *Ann Occup Hyg*; 34: 281–91.
- NIOSH. (1998) What you need to know about occupational exposure to metalworking fluids. NIOSH Publication 98-116, Washington DC: US. Center for Disease Control, <http://www.cdc.gov/niosh/pdfs/98-116.pdf>.
- Paik SY, Vincent JH. (2004) The orientation-averaged aspiration efficiency of IOM-like personal aerosol samplers mounted on bluff bodies. *Ann Occup Hyg*; 48: 3–11.
- Peters TA, Leith D. (2004a) Measurement of particle deposition in industrial ducts. *J Aerosol Sci*; 35: 529–40.
- Peters TM, Leith D. (2004b) Particle deposition in industrial duct bends. *Ann Occup Hyg*; 48: 483–90.
- Piacitelli GM, Sieber WK, O'Brien DM *et al.* (2001) Metalworking fluid exposures in small machine shops: an overview. *AIHAJ*; 62: 356–70.
- Puskar MA, Harkins JM, Moomey JD *et al.* (1991) Internal wall losses of pharmaceutical dusts during closed-face, 37-mm polystyrene cassette sampling. *AIHAJ*; 52: 280–86.
- Roger F, Lachapelle G, Fabries JF *et al.* (1998) Behaviour of the IOM aerosol sampler as a function of external wind velocity and orientation. *J Aerosol Sci*; 29: S1133–34.
- Sabty-Daily RA, Hinds WC, Froines JR. (2005) Size distribution of chromate paint aerosol generated in a bench-scale spray booth. *Ann Occup Hyg*; 49: 33–45.
- Sheehan M. (1999) Final report of the OSHA metalworking fluids. OSHA, Washington DC: Standards Advisory Committee.
- Stear M. (2003) Controlling health risks from workplace to metalworking fluids in the United Kingdom engineering industry. *Appl Occup Environ Hyg*; 18: 877–82.
- Wilsey PW, Vincent JH, Bishop MJ *et al.* (1996) Exposures to inhalable and 'total' oil mist aerosol by metal machining shop workers. *AIHAJ*; 57: 1149–53.
- Witschger O, Grinshpun SA, Fauvel S *et al.* (2004) Performance of personal inhalable aerosol samplers in very slowly moving air when facing the aerosol source. *Ann Occup Hyg*; 48: 351–68.
- Xu M, Willeke K. (1993) Right-angle impaction and rebound of particles. *J Aerosol Sci*; 24: 19–30.
- Zhou Y, Cheng YS. (2010) Evaluation of IOM personal sampler at different flow rates. *J Occup Environ Hyg*; 7: 88–93.